Quantum oscillations of spin polarization in a GaAs/AlGaAs double quantum well

L. Fernandes dos Santos,[1] Yu. A. Pusep,[1] L. Villegas-Lelovsky,[2,3] V. Lopez-Richard,[2] G. E. Marques,[2] G. M. Gusev,[4] D. Smirnov,[5] and A. K. Bakarov[6]

[1]*Instituto de Física de São Carlos, Universidade de São Paulo, 13560-970 São Carlos, SP, Brazil*
[2]*Departamento de Física, Universidade Federal de São Carlos, 13565-905 São Carlos, SP, Brazil*
[3]*Instituto de Física, Universidade de Brasília, 70910-900 Brasília, DF, Brazil*
[4]*Instituto de Física da Universidade de São Paulo, 05315-970 São Paulo, SP, Brazil*
[5]*National High Magnetic Field Laboratory, Tallahassee, Florida 32312, USA*
[6]*Institute of Semiconductor Physics, Novosibirsk, 630090, Russia*

(Received 29 June 2012; revised manuscript received 22 August 2012; published 10 September 2012)

We employ the circular-polarization-resolved magnetophotoluminescence technique to probe the spin character of electron and hole states in a GaAs/AlGaAs strongly coupled double-quantum-well system. The photoluminescence (PL) intensities of the lines associated with symmetric and antisymmetric electron states present clear out-of-phase oscillations between integer values of the filling factor ν and are caused by magnetic-field-induced changes in the population of occupied Landau levels near to the Fermi level of the system. Moreover, the degree of circular polarization of these emissions also exhibits the oscillatory behavior with increasing magnetic field. Both quantum oscillations observed in the PL intensities and in the degree of polarizations may be understood in terms of a simple single-particle approach model. The $\mathbf{k}\cdot\mathbf{p}$ method was used to calculate the photoluminescence peak energies and the degree of circular polarizations in the double-quantum-well structure as a function of the magnetic field. These calculations prove that the character of valence band states plays an important role in the determination of the degree of circular polarization and, thus, resulting in a magnetic-field-induced change of the polarization sign.

DOI: 10.1103/PhysRevB.86.125415 PACS number(s): 73.43.Lp, 73.43.Nq, 78.67.Pt

I. INTRODUCTION

Multiple-layer electron systems are broadly used to explore electronic interaction effects due to a possibility of controlling the competition between intrawell and interwell electron-electron correlations.[1–7] A simplest realization of a multiple-layer system is a double-quantum-well (DQW) structure consisting of two well layers separated by a barrier which provides an important parameter determining the relative contributions of these correlations. When this barrier size becomes narrow enough to enable the strong overlap between carrier wave functions in the bilayer wells, it is possible to control the populations in the symmetric (S) and antisymmetric (AS) subbands. The energy difference, defined as the Δ_{SAS}, can be tuned by changing either the barrier width or height which provides an additional degree of freedom to be explored in this structure.

Although DQW systems have been extensively studied in the literature, experimental investigations are mostly focused on investigation of the many-body effects by means of magnetotransport measurements, as seen in the above references. Inelastic light scattering has also been employed to investigate the interplay between the incompressible and compressible quantum phases of electron bilayers at total filling factor $\nu = 1$.[8] However, and to the best of our knowledge, the polarization-resolved magnetophotoluminescence, which makes possible examining individual responses and populations of the S and AS Landau levels (LL) with different spins, was not yet performed in DQW. This technique can provide information about space and energy distribution of the charge and the spin over the entire electron system.

In a recent work,[7] we explored the strongly coupled GaAs/AlGaAs bilayer system in the range of high-quantized magnetic field, at the filling factor $\nu < 4$, where the quantization of the in-plane kinetic energy results in a considerable interaction among electrons. In this case, the interaction effects lead to the magnetic-field-induced redistribution of charge over the Landau levels that produces the continuous formation of the charge density wave. In this article, we report on the study of polarization-resolved magnetophotoluminescence in the range of quantizing magnetic field, where correlation effects may still be considered negligible and, therefore, the behavior of the bilayer electron system can be accounted for by a single-electron approach. The magnetic-field-induced quantum oscillations of the photoluminescence (PL) intensity and of the degree of circular polarization (DCP) emitted by the S and AS sublevels were demonstrated and analyzed by using the $\mathbf{k}\cdot\mathbf{p}$ method. The role of the electrons and the holes in the observed PL emissions was elucidated.

II. EXPERIMENT

The sample studied here consists of two symmetrical remotely doped GaAs quantum wells with equal well widths, $d = 14$ nm, and separated by a $Al_{0.3}Ga_{0.7}As$ barrier 1.4 nm wide. The high sheet electron density 9×10^{11} cm^{-2}, as measured in Ref. 9, allows occupation of S and AS lowest minibands. Circularly polarized PL measurements were performed at base temperature $T = 300$ mK and in a ^{3}He cryostat with an applied magnetic field perpendicular to the sample surface. The circularly polarized PL spectrum originates from the recombination between electrons with $m_j = \pm 1/2$ and holes $m_j = \pm 3/2$, which occupy a set of lower Landau levels corresponding to the magnetic-field-induced quantization of S and to AS electron and hole states. In order to separate right

(σ^+) and left (σ^-) circularly polarized components, a quarter-wave plate and a linear polarizer setup were placed in front of the sample. The change between the circular polarizations was achieved by reversing the magnetic field direction. The resulting DCP can be determined according to the usual formula $P_\sigma = \frac{I^+ - I^-}{I^+ + I^-}$, where I^+ and I^- are the integrated PL intensities measured in the σ^+ and σ^- polarizations, respectively. It depends on the effective electron-hole (e-h) pair g factor $g_{e\text{-}h} = g_e + g_h$, where g_e and g_h are the electron and hole g factors, respectively.

It should be mentioned that the magnetotransport properties of the sample studied here were extensively investigated in Refs. 9–13 where the reentrant quantum Hall effect, the anisotropic transport, the resonance magnetoresistance oscillations due to electron transitions across the gap between S and AS levels Δ_{SAS}, the effects of interlayer interference, and the microwave zero-resistance states were reported. The presented analysis of the circularly polarized magnetophotoluminescence in coupled bilayers adds important information on the spin character and the coupling between charged carriers which are inaccessible via transport measurements.

III. THEORY

A. Multiband calculation and band-coupling effects

A multiband $\mathbf{k}\cdot\mathbf{p}$ formalism was developed based on the standard Kohn-Luttinger and parabolic Hamiltonian models to probe the electronic structure of holes and electrons, respectively, in this AlGaAs/GaAs bilayer heterostructure.

By considering the coupling between heavy-hole (hh) ($J = 3/2, j_z = \pm 3/2$) and the light-hole (lh) ($J = 3/2, j_z = \pm 1/2$) carriers, where J and j_z denote the band-edge Bloch angular momentum and its z component, the Hamiltonian for the valence band states can be described by

$$\mathcal{H}_h = \mathcal{H}_{\mathrm{KL}} + \left[V_\perp(z) + \mathcal{H}^h_{\mathcal{Z}}\right] I, \tag{1}$$

where $\mathcal{H}_{\mathrm{KL}}$ is the well-known 4×4 Kohn-Luttinger Hamiltonian which takes into account the anisotropic kinetic energy of the valence band carriers in zinc-blende crystals, the $V_\perp(z)$ is the vertical confining potential, and I is the 4×4 identity matrix. Within the multiband effective mass approximation, the kinetic energy of holes is described on the basis of comprised Bloch functions at the top of valence band (Γ_8 point), $|+3/2\rangle, |+1/2\rangle, |-3/2\rangle, |-1/2\rangle$, by the 4×4 Kohn-Luttinger Hamiltonian. When spanned in the j_z spin component basis function, the $\mathcal{H}_{\mathrm{KL}}$ acquires the form

$$\mathcal{H}_{\mathrm{KL}} = \frac{\hbar^2}{m_0}\begin{pmatrix} \mathcal{D}^+_{hh} & \mathcal{A}_- & 0 & \mathcal{B}_- \\ \mathcal{A}^*_- & \mathcal{D}^+_{lh} & \mathcal{B}_- & 0 \\ 0 & \mathcal{B}^*_- & \mathcal{D}^-_{hh} & \mathcal{A}_+ \\ \mathcal{B}^*_- & 0 & \mathcal{A}^*_+ & \mathcal{D}^-_{lh} \end{pmatrix}, \tag{2}$$

where

$$\mathcal{D}_{hh} = -\left(\frac{\gamma_1+\gamma_2}{2}\right)\{\hat{k}_+,\hat{k}_-\} - \left(\frac{\gamma_1-2\gamma_2}{2}\right)\hat{k}_z^2, \tag{3}$$

$$\mathcal{D}_{lh} = -\left(\frac{\gamma_1-\gamma_2}{2}\right)\{\hat{k}_+,\hat{k}_-\} - \left(\frac{\gamma_1+2\gamma_2}{2}\right)\hat{k}_z^2, \tag{4}$$

$$\mathcal{A}_\pm = \mp\sqrt{3}\gamma_3\hat{k}_\pm\hat{k}_z, \tag{5}$$

$$\mathcal{B}_\pm = -\frac{\sqrt{3}}{2}\frac{\gamma_2+\gamma_3}{2}\hat{k}^2_\pm, \tag{6}$$

with $k_\pm = k_x \pm i k_y$, $\mathbf{k} = -i\nabla - e\mathbf{A}/\hbar$, and $\{\hat{k}_+,\hat{k}_-\} = \hat{k}_+\hat{k}_- + \hat{k}_-\hat{k}_+$. Here, m_0 is the electron rest mass, γ_1, γ_2, and γ_3 are the Luttinger-Kohn parameters defining the anisotropic effective masses and the coupling strength between heavy- and light-hole states. Also, $\mathbf{A}$ is the vector potential, which, in the Landau gauge, reads as

$$\mathbf{A} = \mathbf{B}\times\frac{\mathbf{r}}{2} \tag{7}$$

for a magnetic field applied along the growth direction, and which gives rise to a Zeeman energy term

$$\mathcal{H}_{\mathcal{Z}} = -\frac{\hbar e}{m_0}B\left(\kappa J_z + q J_z^3\right). \tag{8}$$

Here, q and κ are the magnetic Kohn-Luttinger parameters which define g factors of holes and where the corresponding matrix elements are stated in the Appendix. The motion in the x direction is now just plane waves, while the y direction corresponds to a one-dimensional (1D) harmonic oscillator. In terms of the raising and lowering operators for the 1D oscillator, the Landau eigenfunctions are easily found to be of the form

$$\Psi^h_v = \sum_{n,s,j_z} C^{j_z}_{n,s}\,\Phi_n(y)h_s(z)\,|j_z\rangle\,, \tag{9}$$

where n is the Landau-level index. Here, the subband eigenfunctions h_s come from the exact solution of the double-square-well potential, taking into account the effective mass mismatch at the GaAs/AlGaAs interfaces (see Ref. 14).

Since the double-quantum-well solutions give rise to symmetric and antisymmetric states, the Hilbert space of the hole wave functions $\Psi^h_v(\mathbf{r})$ can be split into two orthogonal subspaces, with parities which can be compactly labeled as I and II, according to the combination of quantum numbers s and s' in each spinor component. Hence, the eigenvalue problem for the Hamiltonian in Eq. (2) can be solved independently for each class of states I and II. Therefore, the kth-hole wave function (9) with parities I and II can be written as a four-component Kohn-Luttinger spinor

$$\Psi^{I(II)}_k = \sum_s \begin{pmatrix} C^{+\frac{3}{2},k}_{2s-1(2s)}\Phi_{N-2}(y)h_{2s-1(2s)}(z)\left|+\frac{3}{2}\right\rangle \\ C^{+\frac{1}{2},k}_{2s(2s-1)}\Phi_{N-1}(y)h_{2s(2s-1)}(z)\left|+\frac{1}{2}\right\rangle \\ C^{-\frac{3}{2},k}_{2s(2s-1)}\Phi_{N+1}(y)h_{2s(2s-1)}(z)\left|-\frac{3}{2}\right\rangle \\ C^{-\frac{3}{2},k}_{2s-1(2s)}\Phi_{N}(y)h_{2s-1(2s)}(z)\left|-\frac{1}{2}\right\rangle \end{pmatrix}, \tag{10}$$

where h_i are subband functions and C_i are linear combination constants defining the mixture of magnetic oscillator and vertical confining functions. By substituting the expanded wave functions [Eq. (10)] into the eigenvalue problem $(\mathcal{H}_h - E^h_v)\Psi^h_v = 0$, we get the eigenenergies E^h_v and eigenvectors $C^{j_z}_{n,s}$ of hole states. The solution (10) requires us to take the coefficients C_i as zero whenever a Landau index becomes

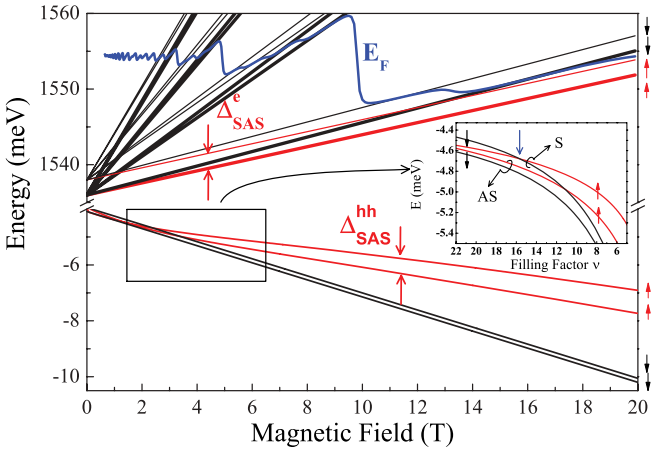

FIG. 1. (Color online) Landau-level fancharts of electron and hole levels calculated for the GaAs/AlGaAs strongly coupled DQW structure defined in the text. The inset shows the energy structure of the valence band for lower energy S and AS states.

negative in a spinor component as, for example, for $N = 0$ the coefficients $C_1 = C_2 = 0$ and, then, leading to a completely uncoupled Landau-level solution. It is clear that the first uncoupled heavy-hole levels correspond to $N = -1$. Meanwhile, the heavy-hole levels with opposite spin orientations belong to the set of full coupled energy levels defined by $N > 2$, which gives rise to the anticrossings between energy levels shown in the inset of Fig. 1.

We treat electrons within the parabolic Hamiltonian model in the effective mass approximation

$$\mathcal{H}_e = \mathcal{H}_0 + \left[V_\perp(z) + \mathcal{H}^e_{\mathcal{Z}}\right] I, \tag{11}$$

where $\mathcal{H}_0 = a^\dagger a$, $\mathcal{H}^e_{\mathcal{Z}} = -g\mu J_z B$, and I is the 2×2 identity matrix. When spanned in the electron Bloch functions, we have a 2×2 diagonal matrix, the elements of which are shown in the Appendix:

$$\mathcal{H}_0 = \begin{pmatrix} \mathcal{H}_0^+ & 0 \\ 0 & \mathcal{H}_0^- \end{pmatrix}. \tag{12}$$

The calculated Landau fanchart diagrams for S and As in the conduction and valence bands of the DQW structure are plotted in Fig. 1. A quantum broadening for the Landau levels of 0.15 meV was taken into account in the Fermi-level calculation $E_F(B)$, and with electron parameters $g_e = -2.6$ and effective mass $m = 0.068m_0$. Both the electron g-factor values, renormalized by correlation effects, and the Landau-level broadening were obtained from the magnetotransport measurements.[9] The best fit of the magnetic field values which match the filling factors corresponding to the polarization peaks was obtained by considering the sheet electron densities $n_S = 4.8 \times 10^{11}$ cm^{-2} and $n_{AS} = 4.4 \times 10^{11}$ cm^{-2} occupying the lowest S and AS levels, respectively.

B. Hole-electron contributions to polarization

In order to determine the DCP, from the theoretical point of view, we must obtain hole and electron occupancies for their corresponding ground states once their product is proportional to the PL intensities. By solving a set of rate equations involving thermal transition processes between the energy states nearest to the top of the valence band, we get

$$h^\pm_\alpha = \frac{2\Theta\left(\pm\Delta^\alpha_h\right) + \zeta^h}{e^{-\frac{|\Delta^\alpha_h|}{K_B T}} + \zeta^h + 1} \tag{13}$$

where

$$\Theta(x) = \begin{cases} 1, & x < 0 \\ e^{-\frac{|x|}{K_B T}}, & x > 0 \end{cases} \tag{14}$$

and $\zeta^h = \tau/\tau^h_s$ is the ratio between τ, the optical recombination time, and the spin-flip time for holes τ^h_s. Here, the indices α label the S and AS states whereas $\pm$ accounts for the spin-up and -down orientations. Finally, K_B is the Boltzmann constant, and Δ^α_h is the Zeeman energy splitting of heavy-hole levels with the same symmetry. In terms of the hole densities, the spin polarization for the S and AS hole states can be written as

$$P^h_\alpha = \frac{h^+_\alpha - h^-_\alpha}{h^+_\alpha + h^-_\alpha}. \tag{15}$$

It is a fact that with the increasing magnetic field, a gradual occupancy of states occurs and it is reflected in the modification of the electron density. Reducing the rate equations for decaying and thermal transition processes for electron yields

$$n^+_\alpha = \frac{\left(\zeta^e + e^{-\frac{\Delta^\alpha_e}{K_B T}}\right) f_+ + e^{-\frac{\Delta^\alpha_e}{K_B T}} f_-}{e^{-\frac{\Delta^\alpha_e}{K_B T}} + \zeta^e + 1}, \tag{16}$$

$$n^-_\alpha = \frac{f_+ + (\zeta^e + 1) f_-}{e^{-\frac{\Delta^\alpha_e}{K_B T}} + \zeta^e + 1}, \tag{17}$$

where f_+ and f_- describe the occupancy of the topmost spin-split levels (fully or partially occupied). Thus, $f_+ = \mathrm{Frac}(\nu)$ (fractional part) and $f_- = 1$, with ν the filling factor. Here, Δ^α_e is the Zeeman energy splitting of the electron levels with the same symmetry and $\zeta^e = \tau/\tau^e_s$ with τ^e_s being the spin-flip time for electrons. Naturally, the particular electron polarization for S and AS states is defined by an expression similar to Eq. (15).

The full polarization turns out a combination of the electron and hole densities

$$P_\alpha = \frac{h^+_\alpha n^+_\alpha - h^-_\alpha n^-_\alpha}{h^+_\alpha n^+_\alpha + h^-_\alpha n^-_\alpha}. \tag{18}$$

It is clear that, in the absence of electron polarization ($n^+_\alpha = n^-_\alpha$), the resulting polarization reduces to the spin polarization of the hole states in Eq. (15). Restricted to the criterion for f_+ and f_-, we can obtain the symmetric and antisymmetric polarizations, respectively, in the domains $(B_{4i+1} + 2, B_{4i})$ and $(B_{4i+3} + 2, B_{4i+2})$ with $B_i = \frac{B_0}{i+1}$.

IV. RESULTS AND DISCUSSION

Figure 2 shows the σ^+ and σ^- PL spectra components measured at 4 T, where the indices S and AS indicate the emissions after recombination between electrons and holes with the same symmetric and antisymmetric parities, respectively. The S and AS contributions were extracted using two Gaussian fits. From these PL spectra we found the energy difference between symmetric-antisymmetric e-h pair

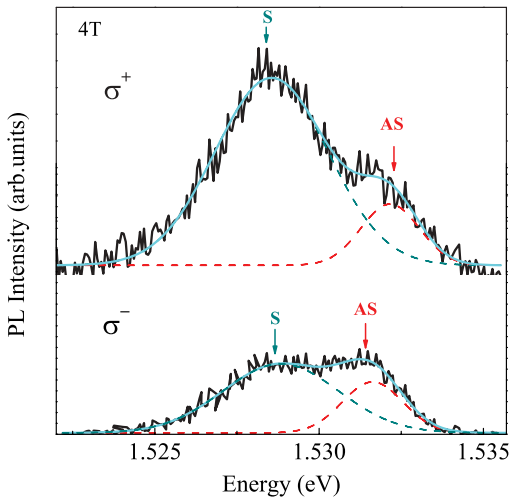

FIG. 2. (Color online) σ^+ and σ^- PL spectra of the GaAs/AlGaAs strongly coupled DQW structure, measured at 4 T. Continuous lines are the best fits using two Gaussian functions for the S and AS emission lines (dashed lines).

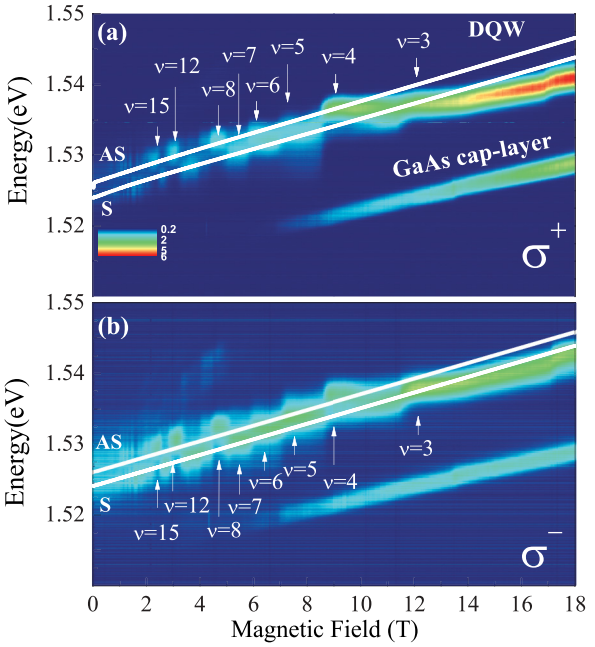

FIG. 3. (Color online) Color-coded maps showing the evolution of the intensity and the energy of the σ^+ (a) and σ^- (b) polarized PL emissions measured as functions of the magnetic field perpendicular to the strongly coupled DQW structure. Continuous white lines are the magnetic field dependencies of the energy emissions, as expected from the *e-h* pair Landau quantization and Zeeman effect.

states $\Delta_{SAS} = 3.6$ and 2.9 meV for σ^+ and σ^-, respectively. Due to the high effective mass value for the heavy holes when compared to the electron mass, the main contribution to the gap Δ_{SAS} comes from electrons. In the absence of the magnetic field, the symmetric-antisymmetric gap for holes is estimated as $\Delta_{SAS} = 0.15$ meV. The *e-h* pair Δ_{SAS} value is found somewhat smaller than the values obtained in magnetotransport measurements ($\Delta_{SAS} = 3.8$ meV) (Refs. 9 and 10) and and in the calculation ($\Delta_{SAS} = 4.2$ meV).

The spectral evolutions of the PL intensity and energy peak position from the strongly coupled DQW are shown by the color-coded maps for σ^+ [Fig. 3(a)] and σ^- [Fig. 3(b)] polarizations as a function of the magnetic field up to 18 T. The four observed PL lines with σ^+ and σ^- polarizations are originated from *e-h* recombination between states with S and AS symmetries and with different spins in order to satisfy the dipole transition selection rules $\Delta S = \pm 1$, respectively. Continuous lines in Figs. 3(a) and 3(b) show the behavior of the PL peak energy expected with the increasing magnetic field, when the Zeeman effect is considered. For magnetic field values corresponding to the filling factor $\nu < 4$, the energies of σ^+ and σ^- polarized emissions deviate from this expected linear dependence. Moreover, in the high magnetic field range, the gap energy Δ_{SAS} decreases and the S and AS lines merge into a single asymmetric PL line. As demonstrated in Ref. 7, such behavior is caused by many-body correlations which become more relevant in the limit of high magnetic fields. In this study, we have focused our attention on the regime $\nu > 4$, when correlation effects become negligible and, therefore, the single-electron approximation used here is still valid.

The detailed magnetic field behaviors of σ^+ and σ^- integrated PL intensities of polarized emissions are shown in Figs. 4(a) and 4(b). Apparent out-of-phase oscillations of these intensity emissions, attributed to transitions between S and AS levels in the DQW structure, were observed with the increasing magnetic field. These oscillations take place at integer filling factors and they are of the same origin as the magnetoresistance (Shubnikov–de Haas) oscillations observed in magnetotransport. They are caused by the magnetic-field-induced quantization of the carrier energies when the magnetic field induces changes in the occupancy of the LLs below the Fermi level. The appearance of the contraphase oscillations of the S and AS intensity emissions is a direct manifestation of the negligibly small symmetric-to-antisymmetric electron scattering. Thus, the S and AS PL emissions are found to be uncoupled, which agrees with similar conclusions recently reported in transport measurements in Ref. 15. Moreover, the oscillations of the PL intensities occur with reference to an average intensity (shown by dashed lines in Fig. 4) of S and AS populations since the total density of electrons in the DQW remains constant, while the magnetic field increase causes the redistribution of the electron density over the S- and AS-occupied Landau levels. It should be mentioned that the oscillations of integrated magnetophotoluminescence intensities have been previously observed in single quantum wells.[16–18] The important difference between a single and a DQW is the formation of a two-component electron system where the S and AS subsystems emit independently.

The DCP determined according to Eq. (1) for the S and AS PL emissions are represented by dots in Figs. 5(a) and 5(b), respectively, and also exhibits an oscillatory behavior with increasing magnetic field. The maxima of DCP are observed at integer filling factors ν. As in the case of the PL intensities discussed above, the peaks of the PL polarization are due to discrete structure of the LLs formed in the conduction band of the bilayer system. Again, the peaks of the DCP associated with the S and AS *e-h* recombinations take place at different filling factors, which is a consequence of the independent S and AS emissions. The peaks in the circular polarization

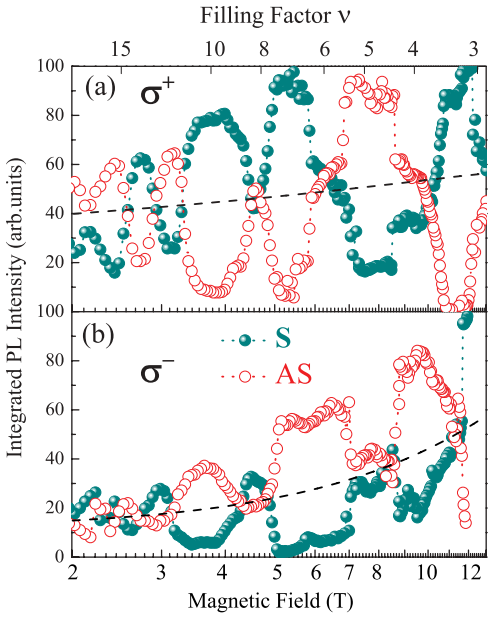

FIG. 4. (Color online) σ^+ (a) and σ^- (b) polarized PL intensities of the DQW structure measured as functions of the magnetic field. Closed (open) circles represent emissions from levels with spacial symmetry S (AS). The dashed curves are guides to the eye, corresponding roughly to the mean value of the polarized PL emission intensity.

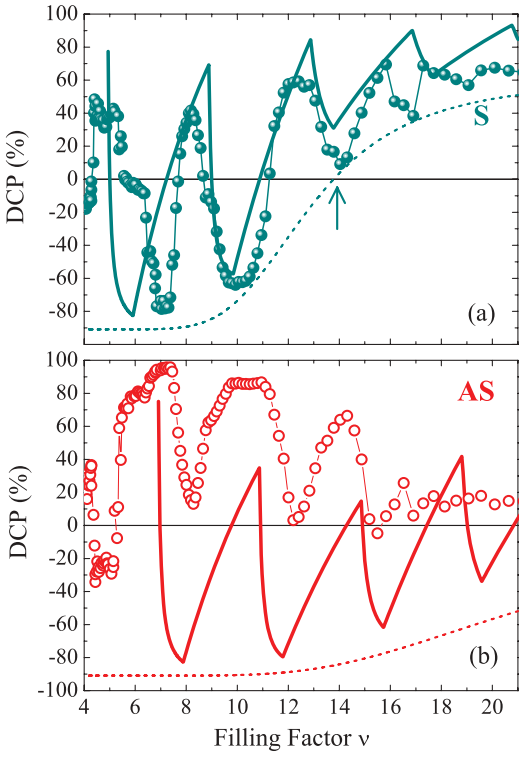

FIG. 5. (Color online) Degree of circular polarization (DCP) as a function of the filling factor ν. Continuous curves represent the calculated DCP for optical interband transitions and dashed curves represent the spin polarization of the occupied hole states: (a) the results corresponding to S and (b) AS levels. The hole polarization inversion for S states is indicated by an arrow in panel (a). In the calculations, the values $\zeta^e = 2$ and $\zeta^h = 0.1$ were used (Ref. 19).

correspond to odd filling factors $\nu = 4N \pm 1$ where N is the LL index and $+$ or $-$ holds for recombination between S and AS states, whereas, at the even filling factors, the electron states are expected to be unpolarized and the total DCP must be completely defined by polarization of the hole states. As stated above, the observed circular polarizations of the PL emissions are associated with the recombinations of *e*-*h* pairs with the effective *g* factor, which have the contributions from electrons and holes. In the calculations of the DCP, we took into account the ground-state heavy holes recombining with the electrons and following strict electric dipole selection rules. In the weak magnetic field range, as shown in Fig. 1, the dependence of the energy of the heavy-hole spin-up valence band states is nonlinear. This results in a crossing between the S spin-up and spin-down heavy-hole energies at the magnetic field near 3 T at the filling factor about $\nu = 15$, whereas no crossing was observed between the AS heavy-hole LL energies. In the inset in Fig. 1, a zoom on the corresponding heavy-hole energies as functions of the filling factor is shown. At the crossing point, as indicated by the arrow in the inset, the contribution of the S heavy holes to the optical polarization changes sign from positive in lower magnetic fields to negative in higher magnetic fields.[19] Dashed lines in Figs. 5(a) and 5(b) show the calculated total spin polarizations of S and AS heavy holes, while solid lines correspond to the total optical polarizations. Indeed, the DCP minima attributed to the transitions between the S states reveal inversion of the sign at the filling factor about $\nu = 15$, indicated by the arrow in Fig. 5(a), while the DCP minima measured for the AS states remain negative in all range of magnetic field, as predicted by the calculations. Thus, as demonstrated in Fig. 5, our calculations reproduce reasonably well the observed magneto-optical oscillations of the DCP, especially at low filling factors, when the LLs are well separated from each other.

V. CONCLUSION

We observed quantum magneto-oscillations of the PL intensities and of the degree of circular polarization associated with the discrete structure of the symmetric and antisymmetric subbands formed in the GaAs/AlGaAs strongly coupled DQW structure in both conduction and valence bands. The distributions of charge and spin over the conduction and valence bands were investigated. Our results show that the symmetric and antisymmetric *e*-*h* pair recombinations take place independently. According to the calculations, the polarization of the holes due to the Zeeman splitting varies monotonically with the magnetic field. The contribution of the heavy holes is responsible for the change in the sign of the PL polarization associated with S states. In turn, the magnetic-field-driven occupancy of the symmetric and antisymmetric conduction band states leads to out-of-phase oscillations of the S and AS emissions between integer filling factors. This confirms that the modulation of structural parameters in nanostructures affects the coupling between heavy- and light-hole subbands[20–22] that, in turn, influences the DCP variation with magnetic field. Thus, we demonstrate that the valence band states play an important role in the circular polarization of the PL emissions in GaAs/AlGaAs strongly coupled DQW structures.

ACKNOWLEDGMENTS

The authors are grateful to the Brazilian agencies FAPESP and CNPq for financial support. D.S. acknowledges support from NHMFL-UCGP and FSU-EEIG programs. Part of this work was performed at NHMFL, which is supported by NSF/DMR- 0654118, the State of Florida, and DOE. We acknowledge fruitful discussions with N. C. Mamani.

APPENDIX: MATRIX ELEMENTS OF THE LANDAU HAMILTONIAN

In terms of matrix elements, we have that full diagonal ($\mathcal{H}^{\pm}_{hh}$ and $\mathcal{H}^{\pm}_{lh}$) and off-diagonal components ($\mathcal{A}_{\pm}$ and $\mathcal{B}_{\pm}$) in Eq. (2) are

$$(\mathcal{H}^{\pm}_{hh})_{n,s,n',s'} = \left[\epsilon^{h}_{s,s'} - (2n'+1)\left(\lambda_{11}\vartheta^{(1)}_{s,s'} + \lambda_{12}\vartheta^{(2)}_{s,s'}\right)B\alpha\tau\right]\delta_{n,n'}\delta_{s,s'} \pm \tfrac{3}{2}\left[\tfrac{9}{4}\left(q_1\vartheta^{(1)}_{s,s'} + q_2\vartheta^{(2)}_{s,s'}\right) + \kappa_1\vartheta^{(1)}_{s,s'} + \kappa_2\vartheta^{(2)}_{s,s'}\right]B\alpha\tau\delta_{n,n'}\delta_{s,s'}, \tag{A1}$$

$$(\mathcal{H}^{\pm}_{lh})_{n,s,n',s'} = \left[\epsilon^{h}_{s,s'} - (2n'+1)\left(\lambda_{11}\vartheta^{(1)}_{s,s'} + \lambda_{12}\vartheta^{(2)}_{s,s'}\right)B\alpha\tau\right]\delta_{n,n'}\delta_{s,s'} \pm \tfrac{1}{2}\left[\tfrac{9}{4}\left(q_1\vartheta^{(1)}_{s,s'} + q_2\vartheta^{(2)}_{s,s'}\right) + \kappa_1\vartheta^{(1)}_{s,s'} + \kappa_2\vartheta^{(2)}_{s,s'}\right]B\alpha\tau\delta_{n,n'}\delta_{s,s'}, \tag{A2}$$

$$(\mathcal{A}_{-})_{n,s,n',s'} = \sqrt{3}\sqrt{B}\sqrt{2n'}\sqrt{\alpha}\tau\delta_{n,n'-1}\left(\gamma_{31}\theta^{(1)}_{s,s'} + \gamma_{32}\theta^{(2)}_{s,s'}\right), \tag{A3}$$

$$(\mathcal{A}_{+})_{n,s,n',s'} = -\sqrt{3}\sqrt{B}\sqrt{2(n'+1)}\sqrt{\alpha}\tau\delta_{n,n'+1}\left(\gamma_{31}\theta^{(1)}_{s,s'} + \gamma_{32}\theta^{(2)}_{s,s'}\right), \tag{A4}$$

$$(\mathcal{B}_{-})_{n,s,n',s'} = \sqrt{3}B\sqrt{n'(n'-1)}\alpha\tau\delta_{n,n'-2}\left(\lambda_{51}\vartheta^{(1)}_{s,s'} + \lambda_{52}\vartheta^{(2)}_{s,s'}\right), \tag{A5}$$

$$(\mathcal{B}_{+})_{n,s,n',s'} = \sqrt{3}B\sqrt{(n'+1)(n'+2)}\alpha\tau\delta_{n,n'+2}\left(\lambda_{51}\vartheta^{(1)}_{s,s'} + \lambda_{52}\vartheta^{(2)}_{s,s'}\right). \tag{A6}$$

In the case of electrons, the matrix elements are

$$(\mathcal{H}^{\pm}_{0})_{n,s,n',s'} = \left[\epsilon^{e}_{s,s'} - \left(n'+\tfrac{1}{2}\right)B\omega\left(\lambda_1\vartheta^{(1)}_{s,s'} + \lambda_2\vartheta^{(2)}_{s,s'}\right)\right]\delta_{n,n'}\delta_{s,s'} \pm \tfrac{1}{2}\left(g_1\vartheta^{(1)}_{s,s'} + g_2\vartheta^{(2)}_{s,s'}\right)B\mu\delta_{n,n'}\delta_{s,s'}, \tag{A7}$$

where $\alpha = e/\hbar$, $\tau = \hbar^2/m_0$. Here, the energy spectrum of the subbands $\epsilon^{(e,h)}_{s,s'}$ was obtained from the transcendental equation,[14] as well subband matrix elements were calculated through numerical integrals, explicitly, for each material region (j = 1-barriers and 2-wells)

$$\Gamma^{(1)}_{p,p'} = \int_{-\infty}^{-\frac{\mathcal{L}}{2}-\ell 1} h^{*}_{p}(z)\hat{A}h_{p'}(z)\,dz + \int_{-\frac{\mathcal{L}}{2}}^{\frac{\mathcal{L}}{2}} h^{*}_{p}(z)\hat{A}h_{p'}(z)\,dz + \int_{\frac{\mathcal{L}}{2}+\ell 2}^{\infty} h^{*}_{p}(z)\hat{A}h_{p'}(z)\,dz, \tag{A8}$$

$$\Gamma^{(2)}_{p,p'} = \int_{-\frac{\mathcal{L}}{2}-\ell 1}^{-\frac{\mathcal{L}}{2}} h^{*}_{p}(z)\hat{A}h_{p'}(z)\,dz + \int_{\frac{\mathcal{L}}{2}}^{\frac{\mathcal{L}}{2}+\ell 2} h^{*}_{p}(z)\hat{A}h_{p'}(z)\,dz, \tag{A9}$$

where $\hat{A} = 1, -\imath\,\partial_z$, respectively for $\Gamma_{p,p'} = \langle p|\hat{A}|p'\rangle = \vartheta_{p,p'}, \theta_{p,p'}$. *It also holds that*

$$\lambda_i\Gamma_{p,p'} = \lambda_{i1}\Gamma^{(1)}_{p,p'} + \lambda_{i2}\Gamma^{(2)}_{p,p'}, \tag{A10}$$

where λ_{ij} are combinations of [100]-direction Kohn-Luttinger parameters: $\lambda_{1j} = \frac{1}{2}(\gamma_{1j} + \gamma_{2j})$,$\lambda_{3j} = \frac{1}{2}(\gamma_{1j} - \gamma_{2j})$, and $\lambda_{5j} = \frac{1}{2}(\gamma_{3j} + \gamma_{2j})$. In a similar way, it is accomplished for the magnetic Kohn-Luttinger parameters q_j and κ_j. The parameters of the GaAs/AlGaAs semiconductor materials were taken from Ref. 23.

[1] G. S. Boebinger, H. W. Jiang, L. N. Pfeiffer, and K. W. West, Phys. Rev. Lett. **64**, 1793 (1990).

[2] A. Sawada, Z. F. Ezawa, H. Ohno, Y. Horikoshi, Y. Ohno, S. Kishimoto, F. Matsukura, M. Yasumoto, and A. Urayama, Phys. Rev. Lett. **80**, 4534 (1998).

[3] V. S. Khrapai, E. V. Deviatov, A. A. Shashkin, V. T. Dolgopolov, F. Hastreiter, A. Wixforth, K. L. Campman, and A. C. Gossard, Phys. Rev. Lett. **84**, 725 (2000).

[4] M. Kellogg, I. B. Spielman, J. P. Eisenstein, L. N. Pfeiffer, and K. W. West, Phys. Rev. Lett. **88**, 126804 (2002).

[5] J. P. Eisenstein and A. H. MacDonald, Nature (London) **432**, 691 (2004).

[6] G. M. Gusev, Yu. A. Pusep, A. K. Bakarov, A. I. Toropov, and J. C. Portal, Phys. Rev. B **81**, 165302 (2010).

[7] Yu. A. Pusep, L. F. dos Santos, G. M. Gusev, D. Smirnov, and A. K. Bakarov, Phys. Rev. Lett. **109**, 046802 (2012).

[8]B. Karmakar, V. Pellegrini, A. Pinczuk, L. N. Pfeiffer, and K. W. West, Int. J. Mod. Phys. B **23**, 2607 (2009).
[9]N. C. Mamani, G. M. Gusev, T. E. Lamas, A. K. Bakarov, and O. E. Raichev, Phys. Rev. B **77**, 205327 (2008).
[10]G. M. Gusev, A. K. Bakarov, T. E. Lamas, and J. C. Portal, Phys. Rev. Lett. **99**, 126804 (2007).
[11]G. M. Gusev, C. A. Duarte, T. E. Lamas, A. K. Bakarov, and J. C. Portal, Phys. Rev. B **78**, 155320 (2008).
[12]S. Wiedmann, G. M. Gusev, O. E. Raichev, A. K. Bakarov, and J. C. Portal, Phys. Rev. Lett. **105**, 026804 (2010).
[13]G. M. Gusev, S. Wiedmann, O. E. Raichev, A. K. Bakarov, and J. C. Portal, Phys. Rev. B **83**, 041306(R) (2011).
[14]L. Villegas-Lelovsky, Fanyao Qu, L. O. Massa, V. Lopez-Richard, and G. E. Marques, Phys. Rev. B **84**, 075319 (2011).
[15]M. Marchewka, E. M. Sheregii, I. Tralle, A. Marcelli, M. Piccinini, and J. Cebulski, Phys. Rev. B **80**, 125316 (2009).
[16]I. V. Kukushkin, K. v. Klitzing, and K. Ploog, Phys. Rev. B **37**, 8509 (1988).
[17]W. Chen, M. Fritze, A. V. Nurmikko, D. Ackley, C. Colvard, and H. Lee, Phys. Rev. Lett. **64**, 2434 (1990).
[18]M. Potemski, Phys. B (Amsterdam) **256–258**, 283 (1998).
[19]L. K. Castelano, D. F. Cesar, V. Lopez-Richard, G. E. Marques, O. D. D. Couto, Jr., F. Iikawa, R. Hey, and P. V. Santos, Phys. Rev. B **84**, 205332 (2011).
[20]E. Margapoti, L. Worschech, S. Mahapatra, K. Brunner, A. Forchel, F. M. Alves, V. Lopez-Richard, G. E. Marques, and C. Bougerol, Phys. Rev. B **77**, 073308 (2008).
[21]E. Margapoti, F. M. Alves, S. Mahapatra, T. Schmidt, V. Lopez-Richard, C. Destefani, E. Menendez-Proupin, Fanyao Qu, C. Bougerol, K. Brunner, A. Forchel, G. E. Marques, and L. Worschech, Phys. Rev. B **82**, 205318 (2010).
[22]E. Margapoti, F. M. Alves, S. Mahapatra, V. Lopez-Richard, L. Worschech, K. Brunner, F. Qu, C. Destefani, E. Menendez-Proupin, C. Bougerol, A. Forchel, and G. E. Marques, New J. Phys. **14**, 043038 (2012).
[23]R. Winkler, *Spin-Orbit Coupling Effects in Two-Dimensional Electron and Hole Systems*, Springer Tracts in Modern Physics (Springer, Berlin, 2003), Vol. 191 and references therein.